

Analyses of the Effect of Inserting Border Lines between Adjacent Color Regions on Detecting Boundaries

경계선 검출에 대한 인접 칼라 영역간 테두리 선 삽입 효과의 분석

유현중*, 김우성**, 장영범*

Hyeon-Joong Yoo*, Woo-sung Kim**, and Young-Beom Jang*

Abstract

This paper presents the analyses of the effect of inserting border lines between different color regions on edge detection in color codes, and is not intended to present any new algorithm for color-code recognition. With its role to complement the RFID (radio frequency identification) and the wide and fast spread of digital cameras, an interest on color codes is fast increasing. However, the severe distortion of colors in obtained images prohibits color codes from expanding their applications. To reduce the effect of color distortion it is desirable to process the whole pixels in each color region statistically, instead of relying on some pixels sampled from the region. This requires segmentation, and the segmentation usually requires edge detection. To help detect edges not disconnected, we inserted border lines of the width of two pixels between adjacent color regions. Two colors were used for the border lines: one consisting of white pixels, and the other black pixels. The edge detection was performed on images with either of the two kinds of border lines inserted, and the results were compared to results without inserted border lines. We found that inserting black border lines degraded edge detection by causing zipper effect while inserting white border lines improved it compared to the cases without inserted border lines.

요약

이 논문은 에지 검출을 위해 다른 컬러 영역사이의 테두리선을 삽입한 효과를 분석한다. 컬러코드를 인식하는 새로운 알고리즘을 제안하지는 않는다. RFID 방식을 보강하고, 디지털 카메라의 이용률이 높아져서 컬러코드에 대한 관심이 매우 증가하고 있다. 그러나 컬러의 왜곡이 심해지면 컬러코드의 확산을 저하시키게 된다. 왜곡된 컬러의 효과를 감소시키기 위해서 영역내 화소 각각의 특성보다 각 영역 전체의 화소를 통계적으로 처리하는 방법이 바람직하다. 이 처리를 위해서 영상 영역화가 필요하다. 연결되지 않은 에지를 검출하기 위해 인접 컬러 영역사이에 2 화소 크기의 테두리선을 삽입한다. 테두리선은 흰색, 검은색 경계선이 사용된다. 2 종류의 테두리선이 삽입된 영상에 대한 에지 검출이 수행되고, 그 결과가 테두리선이 삽입되지 않은 에지 검출 결과와 비교한다. 검은 테두리선을 삽입한 결과는 지퍼효과에 의해 에지 검출 능력이 저하되고, 흰 테두리선을 삽입한 결과는 삽입하지 않은 경우보다 에지 검출 능력이 향상되었다.

Keywords : color code, recognition, edge detection

I. Introduction

Color codes are potentially useful when RFID (radio frequency identification) [1] is too expensive and simple bar coding [2] too rudimentary. Although the barcode and other binary codes [3] are being widely used in managing commercial products, we may benefit from the use of color codes not only in the appearance, but also in the number of combinations. Compared to the RFID, which is receiving drastic attention especially in the areas of ubiquitous computing [4][5] including such projects as u-city and u-government, while they share some application areas, color codes still find their own applications especially for the cases where the RFID can not be employed. And the color code is more economical than RFID solutions and needs no special devices to capture it -- it can be captured by usual camera-equipped cell phones or PC cameras. Independent research shows that, the read-accuracy rate for RFID with multiple tags closely packed together still leaves a lot to be desired--some estimates put accuracy rates as low as 70 percent [5]. Furthermore, RFID is notoriously skittish around metal containers--something to do with metal interfering with the radio signal--which is a considerable drawback in a world where items ranging from soda to motor oil come packaged in metal or metallic materials. Most of all, the RFID is inherently susceptible to fraudulent uses because RF is exposed to anyone, and, for instance, sophisticated EW (Electronic Warfare) technologies [6] might be adversely used to interfere with RFID readers. Table 1 summarizes comparisons among barcode, RFID, and color codes [7].

Table 1 Comparisons of the barcode, RFID, and color code.

표 1 바코드, RFID, 칼라코드의 비교

| | bar code | passive RFID | active RFID | color code |
|--|----------|--------------|-------------|------------|
| Simultaneous multiple asset scanning | | o | o | o |
| Close to 100% reading accuracy | | | o | o |
| Std. data format available today | o | | | o |
| Tag costs less than 5 cents | o | | | o |
| Image bank for visual proof of condition&delivery | | | | o |
| Reads tag from long distances | | | o | o |
| Pin-point indication of non-tagged and non-read assets | | | | o |
| Not affected by RF interference | o | | | o |
| Works with metals present | o | | o | o |
| Works with moisture present | o | | o | o |
| Scans w/o need for manual activation | | o | o | o |
| No line-of-sight requirement | | o | o | |

The fast and wide spread of inexpensive high-resolution digital cameras is also making the application of color codes rapidly expand. There are some companies like Vividot [8], Imedia [9], and ColorzipMedia [10] which allegedly have successfully commercialized color codes: Figs. 1(a) ~ 1(c) show examples of Vividot, Imedia, and ColorzipMedia color code tags, respectively. Figs. 2(a) and 2(b) show some examples of their applications.

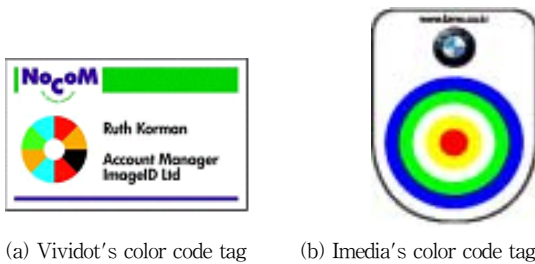
In Fig. 2(a), after photographers have uploaded pictures from an event to the web site of host, visitors to the event visit the website and find their pictures to have them printed [8][9]. Through the procedure, companies not only can pull customers to their websites, but also can have customers experience their online campaign and learn about their customers. This usage can be used to resolve event marketing pains: difficult to measure performance of event marketing activities; limited follow up communication with attendees; and inability to gather comprehensive attendee demographic information. Fig. 2(b) shows another application of color codes where they can be marked on news papers, magazines, or business cards, and they can be taken by using usual PC cameras to

* 상명 대학교 (SangMyung University)

** 호서 대학교 (Hoseo University)

接受日:2006年 5月 8日, 修正完了日: 2006年 6月 15日

be directly linked to a related DB or services [10]. This kind of service is attractive in that it links off-line to on-line. The function that recognizes color codes on off-line products and then links customers to the website that provides related information is expected to encounter increasing demands with the development of various services using color codes.

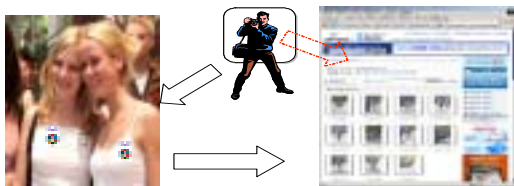


(a) Vividot's color code tag (b) Imedia's color code tag



(c) Colorzip's color code

Fig. 1. color codes.
그림 1. 칼라코드들



(a) Application 1



(b) Application 2

Fig 2. color codes and online services.
그림 2 칼라코드와 온라인 서비스

II. Related Research

However, there are some difficulties in achieving

the practical use of color codes mainly because of the severe distortion of colors. It was observed that the distortion of RGB component values well exceeded over 50% of the whole scale in the obtained RGB images. That might be the major reason why not many companies are launching business using the color code regardless of its advantages, and why there rarely exist any research reports on the subject of color code recognition for which the precise color information is needed, while there are quite a few papers about using rough information of colors to find specific objects like faces [11]-[16].

Figs. 3(a) shows a color code in a tag with a string indicating its colors, and Fig. 3(b) the histograms of it. The segmentation for the figure was performed by handcraft. The upper-most graph in Fig. 3(b) shows the histogram of the hue values of the whole pixels within the circular code region, and the other graphs show the hue histograms for the individual color rings in the order of G, B, M, Y, and B rings. The boxes next to the histograms show the colors obtained by computing the average hue value from each histogram. Notice that the original color code was GBMYB as shown in Fig. 3 (a). Fig. 3 obviously reveals the severity of the degree of color distortion.

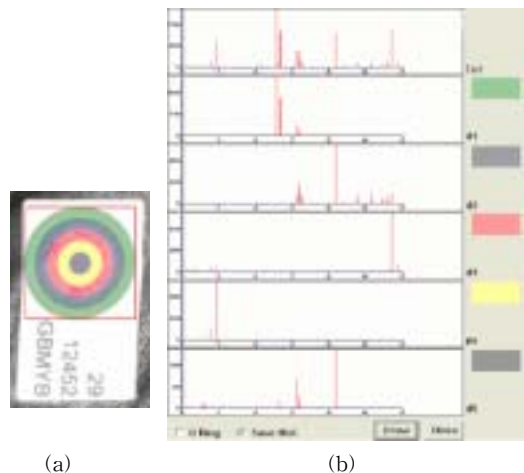


Fig. 3 Histograms of color code region: (a) A color code tag. (The red rectangle is merely a marker in the windows program.) (b) The histograms of the whole

color code region (upper-most) and each color region.

(The boxes in the right column show the colors computed from the histograms. Note that the vertical scales are different.)

그림 3 칼라코드 영역의 히스토그램: (a) 칼라코드 태그.(적색 사각형은 작성한 윈도우 프로그램에서의 마커임.) (b) 칼라코드 영역 전체(맨 위)와 각 칼라 영역별 히스토그램.(우측 박스들은 히스토그램으로부터 계산된 칼라들을 보여줌. 수직 축들의 스케일이 다름에 유의.)

There is also an instrumental distortion that might affect the edge detection. Single-sensor digital cameras spatially sample the incoming image using a color filter array (CFA) [17]. Consequently, each pixel only contains a single color value. In order to reconstruct the original full-color image, a demosaicking step must be performed which interpolates the missing color at each pixel [18]. Demosaicking algorithms usually do well for color fidelity, but there is often a tradeoff between a sharp image and the so-called "zipper-effect" or jagged edge look. The zipper effect may affect the edge detection.

Fig. 4 shows some obscured color code tags cropped from a field image, which show examples of quite usual distortion. Though those who are using the designs of Figs. 1(a) and 1(c) have registered some patents about error checking techniques like parity check, Fig. 4 implies that they are hardly practical and useless without having the code information appear repeatedly on the tag because these signals can not be sent repeatedly. In that sense, the design in Fig. 1(b) is the most practical among them, and, therefore, we choose it for our experiments in this paper.



Fig. 4. Distortion of color codes in field images.

그림 4 필드 영상에서의 칼라코드의 왜곡

In section 2, we explain the edge detection algorithm operated on the concentric color code. And in sections 3 and 4, we perform experiments and compare the effect of inserted black or white border lines on separating different color regions. In section 5, we make conclusion.

III. The Canny Edge Detection

Among the various edge detection techniques, we chose the Canny edge detection because it is known to be the most powerful algorithm. In this section, we briefly introduce the steps of the canny edge detection algorithm [19] used in our experiments:

- (1) Read in parameters (σ , MAG_SCALE, *thr_ratio*, TH, and TL). (These parameters will be explained shortly.)
- (2) Input color image and convert it to gray image I .
- (3) Generate a 1-D Gaussian filter masks G_x and G_y : (The size of the masks is proportional to σ .)

$$G_x = G(x) = e^{-x^2/2\sigma^2}$$

$$G_y = G(y) = e^{-y^2/2\sigma^2}$$

- (4) Take the first derivatives of G along the x- and y-axes to generate 1-D masks G_x' and G_y' :

$$G_x' = G'(x) = -\frac{x}{\sigma^2} e^{-x^2/2\sigma^2}$$

$$G_y' = G'(y) = -\frac{y}{\sigma^2} e^{-y^2/2\sigma^2}$$

- (5) Convolve the image with G_x and G_y to obtain filtered images: (= low pass filtering)

$$I_x = I * G_x$$

$$I_y = I * G_y$$

- (6) Convolve the low-pass filtered images with G_x' and G_y' to obtain gradient images: (= high pass filtering)

$$I_x' = I_x * G_x'$$

$$I_y' = I_y * G_y'$$

- (7) Construct a gradient image by computing the norm of the vertical and horizontal gradient images:

$$I' = \sqrt{(I_x')^2 + (I_y')^2}$$

- (8) Scale the image so that its gray levels span the full gray scale:

$$I'(x,y) = \frac{255}{\max - \min} (I(x,y) - \min) \quad \forall x, y$$

where max and min are the maximum and minimum gray levels in the image I' .

- (9) Multiply the intermediate gradient image by MAG_SCALE (We try 20 and 40 for it) to obtain a gradient image I' :

$$I'(x,y) = \min\{\text{MAG_SCALE} \times I'(x,y), 255\} \quad \forall x, y$$

- (10) Use the nonmaximum suppression method to perform thinning on the edge image.
 (11) Use the hysteresis analysis method with two adaptively chosen threshold values TH and TL to achieve removing isolated edge pixels and joining disconnected edges at a time.

We modify the original algorithm in [19] so that TH and TL are chosen adaptively: i) We first compute the difference between the image size $m \times n$ and the number of pixels with their values of zero in the image from the step 10 as shown in Eq. (3).

$$d = m \times n - h(0) \quad (3)$$

where h stands for the histogram of the nonmaximum-suppressed gradient image and the argument stands for the gray level; ii) Determine the upper-threshold TH by computing the lowest level above which the number of pixels are less than or equal to the difference multiplied by a predetermined factor (i.e., *thr_ratio*) as shown in Eq. (4).

$$\text{TH} = \min_i \{i \mid \sum_{j=i}^{255} h(j) \leq d \times \text{thr_ratio} \text{ for } i \leq 255\} \quad (4)$$

We try 0.3 and 0.7 for *thr_ratio* to investigate opposite cases; iii) Determine the lower-threshold TL to be the average of TH and the first nonzero level after 0 level in the histogram as shown in Eq. (5).

$$\text{TL} = (\text{TH} + \min_i \{i \mid h(i) > 0 \text{ for } i \geq 1\}) / 2 \quad (5)$$

IV. Experiments

In color reading, segmentation is important, but edge detection in color image is usually worse than expected because of color distortions especially

severe at the pixels on the border of adjacent regions of different colors. We explore the effect of white border lines and black border lines inserted between regions of different colors on edge detection.

In the experiments of this paper, we use the design in Fig. 1(b) with the six safe colors, i.e., R, G, B, C, M, and Y. They are chosen because they have equal and the largest distance in hue domain of the HSI color space.

First, we perform the test to see the effect of black border lines inserted between two adjacent color regions. We compare the edge detection results of images using black border lines with those of images not using border lines (Let's call it Experiment I). In Experiment II, we do the comparison for images using white border lines and images not using border lines. The border lines are inserted with the width of two pixels.

In the experiments, we try various shots like waist shot, knee shot, and full shot. And to avoid the effect of characteristics of cameras, we use two different camera models: Nikon and Canon. Both are set to the resolution of 4M pixels. Table 2 shows the number of images used in each experiment for each camera and for each shot category.

Table 2 The numbers of images obtained with each camera in each shot category in each experiment.

표 2 각 실험에서의 촬영 유형 및 카메라별 획득 영상의 수

| Experiment | | I (black) | | II (white) | | Total |
|---------------|-------|-----------|-------|------------|-------|-------|
| | | Canon | Nikon | Canon | Nikon | |
| w/ border | waist | 36 | 36 | 36 | 36 | 144 |
| | full | 36 | 36 | 36 | 36 | 144 |
| w/o border | waist | 36 | 36 | 36 | 36 | 144 |
| | full | 36 | 36 | 36 | 36 | 144 |
| Total | | 144 | 144 | 144 | 144 | 576 |

* The waist, knee, and full stand for the shot types.

Figs. 5(a) and 5(b) show a test image of waist shot and a color-code region cropped from it by handcraft, respectively.

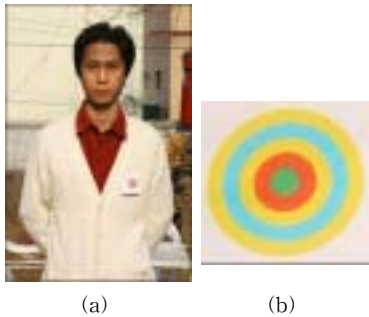


Fig. 5 A test image of waist shot and the cropped color-code region from it.

그림 5 웨이스트 샷 시험영상과 그로부터 추출된 칼라코드 영역

We apply Canny edge detector to the gray image of the cropped color-code image. To find the proper values of the major parameters of the edge detection algorithm, we perform pilot tests with eight different combinations of parameters as shown in Table 3 using some randomly selected images. Two values are chosen for each parameter so that they have opposite effects on the image.

Table 3 The eight combinations of parameters of the Canny edge detector.

표 3 캐니 경계선 검출기 파라미터들의 8가지 조합

| para. | sigma | MAG_SCALE | thr_ratio |
|-------|-------|-----------|-----------|
| 1 | 2 | 20 | 0.3 |
| 2 | 2 | 20 | 0.7 |
| 3 | 2 | 40 | 0.3 |
| 4 | 2 | 40 | 0.7 |
| 5 | 5 | 20 | 0.3 |
| 6 | 5 | 20 | 0.7 |
| 7 | 5 | 40 | 0.3 |
| 8 | 5 | 40 | 0.7 |

V. Experimental Results and Analyses

Fig. 6 shows an example of the edges detected using the eight combinations of parameters in Table 3. The first image on the left top is the color code

cropped from a field image. The next one in the same row corresponds to the first parameter combination in Table 3, and so on. This figure shows that the parameter combinations 2, 4, and 8 gave the best edge detection performance for the Canny algorithm in this application. Since this result was typical for almost all test images, we used these three parameter combinations for the next comparison experiments.

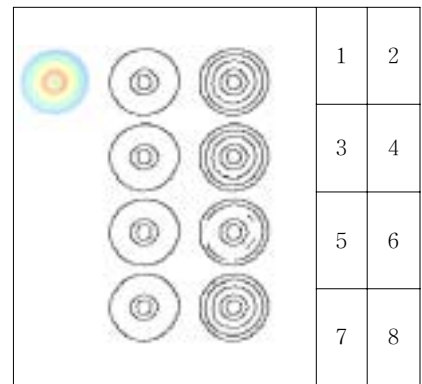


Fig. 6 The edge images obtained by applying Canny edge detector with the eight combinations of parameters shown in Table 3 to the color code from a field image. (The numbers in the last two columns correspond to the parameter combination indices in Table 3.)

그림 6 필드 영상으로부터의 칼라코드에 대해 표 3의 8 가지 파라미터 조합으로 캐니 경계 검출기를 적용해서 얻은 경계선 영상들(끝 두 열의 숫자들은 표 3의 파라미터 조합 인덱스에 해당)

Tables 4 and 5 show the results obtained by using those three parameter combinations for Experiments I and II, respectively. Each real number represents in percentage the ratio of the number of edge pixels detected in the cropped image to the size of it. The values in columns from 3 to 5 correspond to the parameter combinations 2, 4, and 8, respectively. The values in the last column shows the average in each row.

Table 4 The comparison between the results with black border lines inserted and the results without inserted border lines (Experiment I)

표 4 흑색 테두리 선을 삽입했을 때와 삽입하지 않았을 때의 결과 비교(실험 I)

| Shot | border | para. 2 | para. 4 | para. 8 | mean |
|-------|--------|---------|---------|---------|--------|
| Canon | | | | | |
| full | w/ | 15.147 | 15.289 | 14.364 | 14.934 |
| | w/o | 15.166 | 15.367 | 15.899 | 15.477 |
| waist | w/ | 11.215 | 11.507 | 10.296 | 11.006 |
| | w/o | 11.551 | 11.699 | 10.317 | 11.189 |
| Nikon | | | | | |
| full | w/ | 13.557 | 13.581 | 14.200 | 13.779 |
| | w/o | 14.657 | 14.629 | 12.202 | 13.829 |
| waist | w/ | 11.699 | 11.699 | 10.927 | 11.442 |
| | w/o | 14.352 | 14.355 | 13.973 | 14.226 |

Table 5 The comparison between the results with white border lines inserted and the results without inserted border lines (Experiment II)

표 5 백색 테두리 선을 삽입했을 때와 삽입하지 않았을 때의 결과 비교(실험 II)

| Shot | border | para. 2 | para. 4 | para. 8 | mean |
|-------|--------|---------|---------|---------|--------|
| Canon | | | | | |
| full | w/ | 13.713 | 13.772 | 13.408 | 13.631 |
| | w/o | 12.089 | 12.490 | 11.529 | 12.036 |
| waist | w/ | 10.826 | 10.857 | 9.047 | 10.243 |
| | w/o | 10.193 | 10.216 | 8.079 | 9.496 |
| knee | w/ | 12.896 | 13.084 | 12.569 | 12.850 |
| | w/o | 11.297 | 11.642 | 10.112 | 11.017 |
| Nikon | | | | | |
| full | w/ | 13.220 | 13.340 | 13.368 | 13.309 |
| | w/o | 10.188 | 10.592 | 9.718 | 10.166 |
| waist | w/ | 10.514 | 10.635 | 9.022 | 10.057 |
| | w/o | 10.452 | 10.271 | 7.146 | 9.290 |
| knee | w/ | 12.196 | 12.644 | 11.931 | 12.257 |
| | w/o | 10.917 | 11.017 | 8.953 | 10.296 |

Table 4 shows that the cases using black border lines almost always provided lower edge detection ratios than those without using border lines; Table 5 shows that the cases using white border lines always provided higher edge detection ratios than those without using border lines. Based on these observations, we may conclude that inserting black border lines gives adverse effect on detecting edges

between adjacent color regions, while inserting white border lines yields favorable effect.

VI. Discussion

As can be seen in Table 3, the three best combinations 2, 4, and 8 share the same *thr_ratio* of 0.7, which means that the upper-threshold value (TH) for the hysteresis analysis phase can be far below the median among the nonzero pixel values. On the other hand, the low value of *thr_ratio* led to the high value of TH, which resulted in missing even some important edges.

As the value of the parameter sigma, σ , of the Canny algorithm became larger, the Gaussian lowpass filter has narrower bandwidth, which resulted in blurring edges. Hence we would have to use a larger MAG_SCALE factor for a lowpass-filtered image obtained with a larger sigma than with a smaller sigma. That explains how come the second and the eighth parameter combinations in Table 3 showed comparable performance to each other.

VII. Conclusion

In this paper, we analyzed the effect of inserting border lines of either black or white colors between adjacent color regions. We compared the results to those without inserted border lines. We found that black border lines gave adverse effect, while white border lines improved the edge detection. This observation is meaningful in that it will help separate different color regions from each other, which will eventually allow us to get more accurate color reading by enabling us to statistically process each color region using its entire pixels, instead of using some regularly sampled pixels from the region.

References

- [1] Robertson and Jaialy, "RF id tagging explained", *Communications Engineer*, vol. 1, pp. 20-23, 2003.
- [2] T. Pavlidis, J. Swartz, and Y. Wang, "Fundamentals of bar code information theory", *IEEE Computer*, vol. 23, pp. 74-86, 1990.
- [3] <http://www.hitl.washington.edu/artoolkit>
- [4] *Ubiquitous market forecast report*, ISBN: 89-89861-48-9 94500, Strategic Technology Management Institute (STEMI), Nov. 2004.
- [5] H. Atkinson, "Coming soon to a container near you?", *DC Velocity*, pp. 47-49, March 2005.
- [6] S. Vakin, L. Shustov, and R. Dunwell, *Fundamentals of electronic warfare*, Artech House Publishers, June 2001.
- [7] "AIDC technology matrix", <http://www.visidot.com>
- [8] <http://www.vividot.com>
- [9] <http://print.imedia.co.kr>
- [10] <http://www.colorzip.com>
- [11] C. Garcia and G. Tziritas, "Face detection using quantized skin color regions merging and wavelet packet analysis", *IEEE Transactions on Multimedia*, vol. 1, no. 3, 1999.
- [12] M. Jones and J. Rehg, "Statistical color models with application to skin detection", *Cambridge Research Laboratory Technical Report Series*, 1998.
- [13] K. Sobottak and Pitas, "Extraction of facial regions and features using color and shape information", *IEEE Int. Conf. on Pattern Recognition*, vol. 3, Aug. 1996.
- [14] D. Chai and K. Ngan, "Face segmentation using skin-color map in videophone applications", *IEEE Trans. on Circuits and Systems for Video Technology*, vol. 9, no. 4, 1999.
- [15] J. Park, J. Seo, D. An, and S. Chung, "Detection of human faces using skin color and eyes", *Proceeding of IEEE Int. Conf. on Multimedia and Expo*, vol. 1, pp. 133-136, 2000.
- [16] S. Shin and S. Choi, "Fast face detection in video using the HCr and adaptive thresholding method", *Trans. of IEEE*, vol. 41, no. SP-6, Nov. 2004.
- [17] W. Lu and Y. Tan, "Color filter array demosaicking: New method and performance measures", *IEEE Trans. Image Processing*, vol. 12, no. 10, pp. 1194-1210, 2003.
- [18] R. Ramanath, W. Snyder, and G. Bilbro, "Demosaicking methods for Bayer color arrays", *J. Electronic Imaging*, vol. 11, pp. 306-315, 2002.
- [19] J. R. Parker, *Algorithms for Image Processing and Computer Vision*, Wiley, 1997.

저자 소개

김우성 (정회원)



1980년 서강대학교(학사)
1993년 서강대학교(박사)
1984년~1987년 한국전자통신연구원
1999년~2000년 미국 Univ. of Washington 연구 교수
1987년~현재 호서대학교 컴퓨터학부 교수
2003년~현재 호서대학교 첨단정보

기술대학원장, 뉴미디어연구소장
2006년~현재 호서대학교 정보관리처장
<주관심분야>
멀티미디어, 영상처리, 무선인터넷

장영범 (정회원)



1981년 : 연세대학교 전기공학과 졸업 (공학사)
1990년 : Polytechnic University 대학원 전기공학과 (공학석사)
1994년 : Polytechnic University 대학원 전기공학과 (Ph.D.)
1983년 ~ 1999: 삼성전자 시스템LSI사업부 수석연구원

2002년 ~ 현재 : 상명대학교 정보통신공학과 교수
주관심분야 : 신호처리, SoC설계

유현중 (정회원)



1982년 : 서강대학교 전자공학과 졸업 (공학사)

1991년 : 미주리 대학교 전기및컴퓨터공학과
(공학석사)

1996년 : 미주리 대학교 전기및컴퓨터공학과
(Ph.D.)

1996년 ~ 현재 : 상명대학교 정보통신공학과 교수

<주관심분야>

패턴인식, 영상처리